Lumbar Instability Induces Ligamentum Flavum Hypertrophy in a Rat Model

Baojian Wang
Department of Spine, Wangjing Hospital of China Academy of Chinese Medical Sciences, Beijing, China
Chunyu Gao
Department of Spine, Wangjing Hospital of China Academy of Chinese Medical Sciences, Beijing, China
Liguo Zhu
Department of Spine, Wangjing Hospital of China Academy of Chinese Medical Sciences, Beijing, China
Ping Zhang
Department of Pathology, Wangjing Hospital of China Academy of Chinese Medical Sciences, Beijing, China
Wu Sun
Department of Spine, Wangjing Hospital of China Academy of Chinese Medical Sciences, Beijing, China
Jingru Zhang
Department of Pathology, Wangjing Hospital of China Academy of Chinese Medical Sciences, Beijing, China
Jinghua Gao (✉ gaojinghua2019@hotmail.com)
Department of Spine, Wangjing Hospital of China Academy of Chinese Medical Sciences, Beijing, China
Xu Wei
Office of Academic Research, Wangjing Hospital of China Academy of Chinese Medical Sciences, Beijing, China

Research Article

Keywords: experimental study, ligamentum flavum, hypertrophy, lumbar instability, inflammatory factor, fibrotic factor, immunohistochemistry, real-time PCR, Masson trichrome staining, lumbar degenerative disease, rat model

Posted Date: January 8th, 2021

DOI: https://doi.org/10.21203/rs.3.rs-140228/v1

Version of Record: A version of this preprint was published at BMC Musculoskeletal Disorders on April 6th, 2021. See the published version at https://doi.org/10.1186/s12891-021-04203-x.

Lumbar instability induces ligamentum flavum hypertrophy in a rat model

Baojian Wang[1△], Chunyu Gao[1△], Liguo Zhu[1], Ping Zhang[2], Xu Wei[3], Wu Sun[1], Jingru Zhang[2], Jinghua Gao[1]*

[1]Department of Spine, Wangjing Hospital of China Academy of Chinese Medical Sciences, Beijing, China
[2]Department of Pathology, Wangjing Hospital of China Academy of Chinese Medical Sciences, Beijing, China.
[3]Office of Academic Research, Wangjing Hospital of China Academy of Chinese Medical Sciences, Beijing, China

*Corresponding author: Jinghua Gao E-mail: gaojinghua2019@hotmail.com
△: Baojian Wang and Chunyu Gao contributed equally to this work.

Abstract

Background: The purpose of this study was to establish a novel rat model for ligamentum flavum (LF) hypertrophy using lumbar instability and to elucidate the etiology of LF hypertrophy.

Methods: A total number of 30 male rats were used. Lumbar instability was induced by surgical resection of L5/6 posterior elements (n=15). The other rats underwent a sham operation (n=15). After 8 weeks, all rats were taken lateral plain X-rays. The LF from L5/6 in both groups were harvested to investigate histological, immunohistological, and real-time PCR analysis.

Results: According to radiological results, the disc height ratio and extension ratio were larger in the rats in the experimental group than that of in the control group. The HE staining showed that the LF thickness in the experimental group significantly increased in comparison to the control group. The Masson trichrome staining showed that the ratio of elastic fibers to collagen fibers in experimental group was lower than that in the control group. The protein and gene expression of TGF-β1, TNF-α, IL-1β, and Col 1 were significantly higher in the experimental group than that in the control group.

Conclusion: It is the first time that lumbar instability directly induced LF hypertrophy in a reproducible rat model. Lumbar instability could lead to high expression of inflammatory and fibrotic factors in LF, causing the accumulation of collagen fibers and decreasing of elastic fibers.

Keywords: experimental study, ligamentum flavum, hypertrophy, lumbar instability, inflammatory factor, fibrotic factor, immunohistochemistry, real-time PCR, Masson trichrome staining, lumbar degenerative disease, rat model.

Background

Lumbar spinal canal stenosis (LSCS) is a common spinal disorder in elder people causing low back pain, gait disturbance, leading to severe disability in the activities of daily living [1]. There are approximately 250,000 to 500,000 LSCS patients in the United States [2]. In these patients with LSCS, protruded lumbar discs, hypertrophied ligamentum flavum (LF) and bulged facet joints compress the dural sac, cauda equine, or nerve-roots, leading to canal narrowing (stenosis). Because the LF covers most of the posterior and lateral parts of the spinal canal. The cauda equine or nerve roots can be mechanically compressed by hypertrophy LF, resulting in spinal symptoms [3]. Although numerous investigations have been conducted to clarify the degeneration of the LF in LSCS patients using the tissue harvested during spine surgery [4]. The hypertrophied LF of human already showed a common histological changes: the loss of elastic fibers and an excessive accumulation of collagen fibers [5-6]. In addition, molecular overexpression were also found in human hypertrophied LF. The inflammatory factors such as Interleukin-1 (IL-1β), Tumor Necrosis Factor (TNF-α), and fibrogenic cytokines such as Transforming Growth Factor-β1 (TGF-β1) were observed [8-9]. However, whether such factors are causative or merely a consequence of LF hypertrophy remains unknown. The exact molecular mechanism of LF hypertrophy has not been revealed yet [10-11]. Therefore, basic research using an experimental animal model is necessary to clarify its pathomechanism.

In clinical situations, lumbar instability is frequently observed in patients with LSCS, and this changes might have a positive correlation with its pathogenesis [12]. Fukuyama et al [13] found that the LF thickness of lumbar instability patients was larger than that of non-instability patients. Several experimental animal models of intervertebral disc degeneration resulted from spinal instability have been reported [14-16]. However, there are no basic studies applying an experimental animal directly demonstrating that lumbar instability induces LF hypertrophy.

Therefore, in this study, we aimed to establish a novel rat model for degeneration and hypertrophy of the LF using lumbar instability. We also intended to investigate the effect of lumbar instability on LF degeneration to elucidate the etiology of LF hypertrophy.

Methods

Animals and groups

Thirty eight-week-old male Sprague-Dawley rats, each weighing about 250g were used. During the experiment, all rats were housed in a temperature- and humidity-controlled environment with a 12h light/12h dark cycle. All experiments were approved by the Animal Ethics Committee of the Institute of Basic Theory for Chinese Medicine, China Academy of Chinese Medical Sciences and were compliant with NIH guidelines for the humane care and use of laboratory animals. All methods were carried out in accordance with ARRIVE guidelines. During surgical procedures, the rats were anesthetized by an intraperitoneal injection of sodium pentobarbital (50mg/kg), given injection of antibiotics (20mg/kg of Cefuroxime Sodium; Medochemie, Cyprus) and then operated aseptically throughout the experiments. They were randomly divided into two groups. To obtain lumbar instability on in L5/6 level, the first group (group A; n=15) underwent complete resection of L5 and L6 spinous process, semi-grinding (Grinder, Seashin 204, Daegu, Korea) of the bilateral L5/6 facet joints, and removal of L5-L6 paraspinal muscle (Fig. 1a-c). The second group (group B; n=15) just underwent surgical exposure as a sham operation. All rats were received food pellets and water ad libitum. Two groups of rats were sacrificed at 8 weeks after surgery.

Radiological analysis

Eight weeks after operation, all rats were taken lateral plain X-rays of the lumbar spine under general anesthesia by an intraperitoneal injection of sodium pentobarbital (50 mg/kg). To ensure the same degree of extension and flexion in all rats, a simple retractable holder was constructed to make sure consistent distance from the head to the tail (Fig. 1d). The lumbar instability reflected by disc height and mobility of the L5/6 segment were gauged using Image J 1.50 software (National Institutes of Health) and were compared between two groups [13,16] (Fig. 1e).

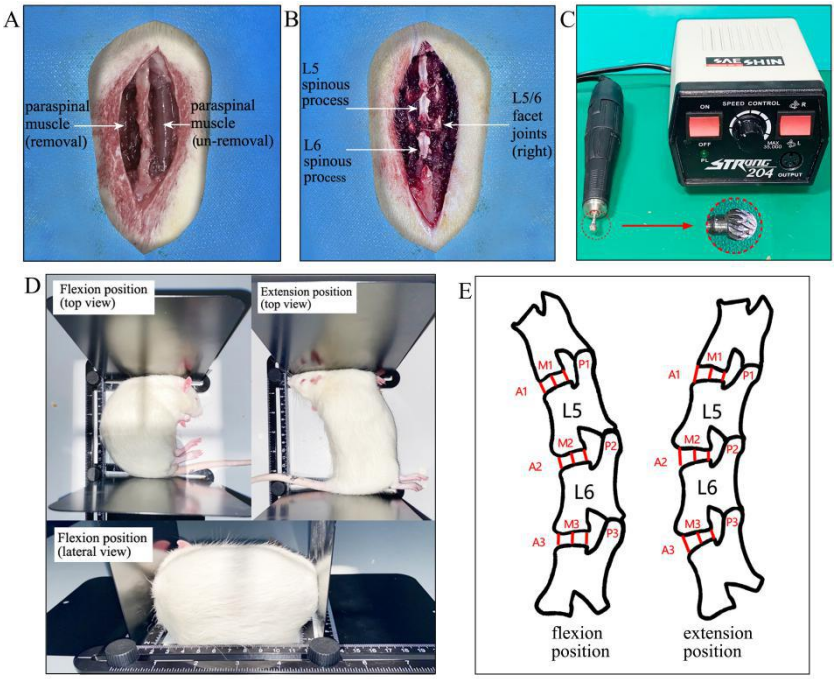

Fig 1. Surgical procedures and radiological methods. (A) Removal of L5-L6 paraspinal muscle. (B) Complete resection of L5 and L6 spinous process, semi-grinding of the bilateral L5/6 facet joints. (C) A Grinder and round drill bit used to semi-grind the facet joints. (D) Over extension and flexion position of rats using a retractable holder. (E) Measurement indicators: (1) Disc height ratios (DHR) in flexion and extension were calculated as follows: anterior DHR = 2×A2/(A1+A3), middle DHR = 2×M2/(M1+M3), posterior DHR = 2×P2/(P1 + P3). (2) Flexion and extension ratios were calculated as follows: flexion ratio = A2/P2 in flexion, extension ratio = A2/P2 in extension. A anterior, M middle, P posterior.

Human LF samples

Human LF was collected at surgery from 10 lumbar disc herniation (LDH) patients (mean age 41.2 years, range 26–55 years, LF < 4 mm, as non-hypertrophied LF) and 10 LSCS patients (mean age 54.7 years, range 51–71 years, LF ≥ 4 mm, as hypertrophied LF) who had undergone decompressive laminectomy. The thickness of human LF was measured at the facet joint level on axial T2-weighed magnetic resonance imaging (MRI) [17]. These sections were prepared to Masson staining. All procedures were approved by the Ethics Committee of Wangjing hospital, Chinese Academy of traditional Chinese Medicine (WJEC-YJS-2020-009-P002) and all procedures were performed according to the Declaration of Helsinki. All patients received written informed consent before operation. The LF was collected during surgery after obtaining the informed consent from patients.

Histological analysis and immunohistological evaluation

The lumbar spinal without any muscles were cut along the coronal plane at the intervertebral foramen to separate them into the anterior and posterior spine column. The posterior lumbar spinal with the LF on the left side were harvested and fixed with 4% paraformaldehyde phosphate buffer solution for 48 hours. Then this posterior lumbar spinal was decalcified in 10% ethylenediaminetet raacetic acid (EDTA) solution for eight weeks. The L5/6 posterior lumbar spinal were sliced along the cross plane at the facet joint level. These samples were embedded in paraffin and sliced in to 4 μm. This sections were subjected to hematoxylin-eosin (HE) and Masson trichrome (MT) staining. MT staining was to distinguish between collagen fibers (blue) and elastic fibers (red). Ligaments in the human specimens were processed as above without to be decalcified. The Image J 1.50 software was used to measure the area, thickness, width, and the area of collagen or elastic fiber of the rat LF at the L5/6 facet joint level

on the axial sections.

For immunostaining, the sections were retrieved with EDTA retrieval buffers (PH 9.0; Wuhan Boster Biological Technology Ltd., Wuhan, China) at 100 ℃ for 30 min. Endogenous peroxidase activity was quenched in 3% H_2O_2 for 30 min, and endogenous immunoglobulin was then blocked with 3% bovine serum albumin (Beijing Solarbio Science & Technology, Co., Ltd., Beijing, China) for 30 min. After incubation with TGF-β1 rabbit monoclonal antibody (1:50; Beijing Bioss Biological Technology Ltd., Beijing , China), TNF-α antibody rabbit polyclonal antibody (1:100; Wuhan Boster Biological Technology Ltd., Wuhan, China), IL-1β rabbit monoclonal antibody (1:200; Beijing Bioss Biological Technology Ltd., Beijing, China), and Col 1 rabbit monoclonal antibody (1:100; Beijing Bioss Biological Technology Ltd., Beijing, China) for 2 hours, the secondary antibody (1:100; Beijing Bioss Biological Technology Ltd., Beijing, China) incubation was carried out for 2 hour. The reaction was visualised using the DAB. The sections were counters-tained using hematoxylin. The mean optical density (MOD) of positive cells was analysed in the axial sections at the L5/6 facet joint level using Image J 1.50.

RNA isolation and real-time PCR Analysis

After the rats were sacrificed, the LF of the right side from L5/6 were stored in liquid nitrogen immediately. According to the manufacturer's instructions, total RNA was isolated from LF tissue using a total RNA preparation kit (Axygen, NY, USA) and cDNA was synthesized from the total RNA using a PrimeScript reverse transcriptase (TAKARA, Shiga, Japan). Relative mRNA expression was determined using RT-PCR with the GoTaq 1-step RT-qPCR system (TAKARA), agarose gel electrophoresis system (BioRad, CA, USA) and qPCR using SYBR premix Ex Taq kit (TAKARA) with ABI Prism 7500 Fast Real-Time PCR system (Applied Biosystems, Foster City, CA). Gene expression was quantified using the $2^{-\triangle\triangle CT}$ method. GAPDH was used as an internal control. The primer sequences of genes were obtained from Primer Bank. All the primers were synthesized by Servicebio Biotech (Wuhan, China). For real-time PCR, the primers were synthesized as follows: GAPDH, 5'-AAGAAGGTGGTGAAGCAGG-3' (forward) and 5'- GAAGGTGGAAGAGTGGGAGT-3' (reverse); TGF-β1, 5'-CCTGTCCAAACTAAGGCTCG-3' (forward) and 5'-ATGGCGTTGTTGCGGTC-3' (reverse); IL-1β, 5'-GGGCTGGACTGTTTCTAATGCCTT-3' (forward) and 5'-CCATCAGAGGCAAGGAGGAAAACA-3' (reverse); TNF-α, 5'-TTATGGCTCAGGGTCCAACTCTGT-3' (forward) and 5'-TGGACATTCGAGGCTCCAGTGAAT-3' (reverse);
Col 1, 5'-AACCCTGGAAACAGACGAACAACC-3' (forward) and 5'-TGGTCACGTTCAGTTGGTCAAAGG-3' (reverse).

Statistical analysis

All statistical analyses were performed with SPSS 22.0 (IBM Corp., Armonk, NY, USA). Student's t-test and Mann-Whitney U test were respectively used to compare the radiographical and histological scores between the surgery and sham groups. p values$<$0.05 were considered significant.

Results

Radiological analysis

According to the radiological results, the rats of experimental group showed wide disc space and bone spurs of the anterior vertebral rims at the L5/6 level. The L5 and L6 spinous processes of all rats were still absent, but the L5/6 facet joints returned to normal as the other sham rats. No slippage of the vertebral body was seen at at the L5/6 level (Fig. 2a-b). Additionally, the disc height ratio and extension ratio were larger in the rats in the experimental group than that of in the control group (Fig. 2c-e). These results reflected that the intervertebral disc height in dynamic position and the motion range of flexion and extension increased, leading to spinal instability at the surgical segments.

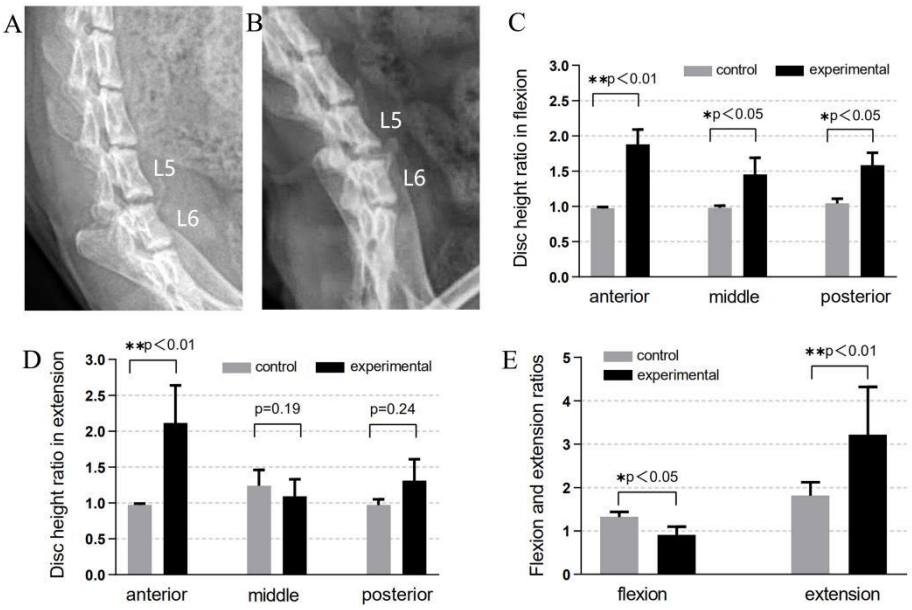

Fig 2. Radiological analysis at 8 weeks postoperatively. Wide disc space and anterior osteophyte formation was found on L5/6 of (A) flexion position and (B) flexion position on lateral radiographs. (C) The disc height ratio of the flexion position was larger in the rats in the experimental group than in the rats in the control groups. (D) The anterior disc height ratio of the extension position was larger in the rats in the experimental group than in the rats in the control groups. (E) The extension ratios were larger in the rats in the experimental group than in the rats in the control groups.

Lumbar instability induced LF hypertrophy

In order to test whether lumbar instability indeed brought about LF hypertrophy, we compared the L5/6 axial cross-sectional pathological section of all rats. After 8 weeks, The HE staining showed that the thickness of the experimental group was 656±21.4 μm, which was significantly higher than that of the same level in control group ($p < 0.05$). The width of two groups had no distinct difference ($p=0.08$). The axial cross-sectional area in the experimental group was about 1.33-fold that of the same level in control group ($p<0.05$, Fig. 3a-f).

Then we examined the effect of lumbar instability on the extracellular matrix (ECM) of the rat LF by MT staining. Previous studies had demonstrated that the ECM of human non-hypertrophied LF was mainly composed of major elastic fibers and minor collagen fibers. However the proportion of collagen fibers was accordingly increased when LF hypertrophied [5-6]. Our experiment showed similar results. The ratio of elastic fibers to collagen fibers in experimental group was lower than that in the control group ($p < 0.05$). Although the area of elastic fibers also increased, the density of elastic fibers decreased (Fig. 3g-n) .

In addition, a fibrotic area was found at the HF dorsal aspect layer in the experimental group (Fig. 3g, red circle). This fibrotic area mainly composed of collagen fibers on MT staining. The mean thickness of this enlarged dorsal layer of HF was 159±8.37 μm in experimental group, which was notably thicker than in the control rat (Fig. 3i, red circle).

These results indicated the successful establishment of a LF hypertrophy rat model by lumbar instability. On the other hand, posterior destabilization of lumbar could also cause enlargement of the dorsal side of the LF.

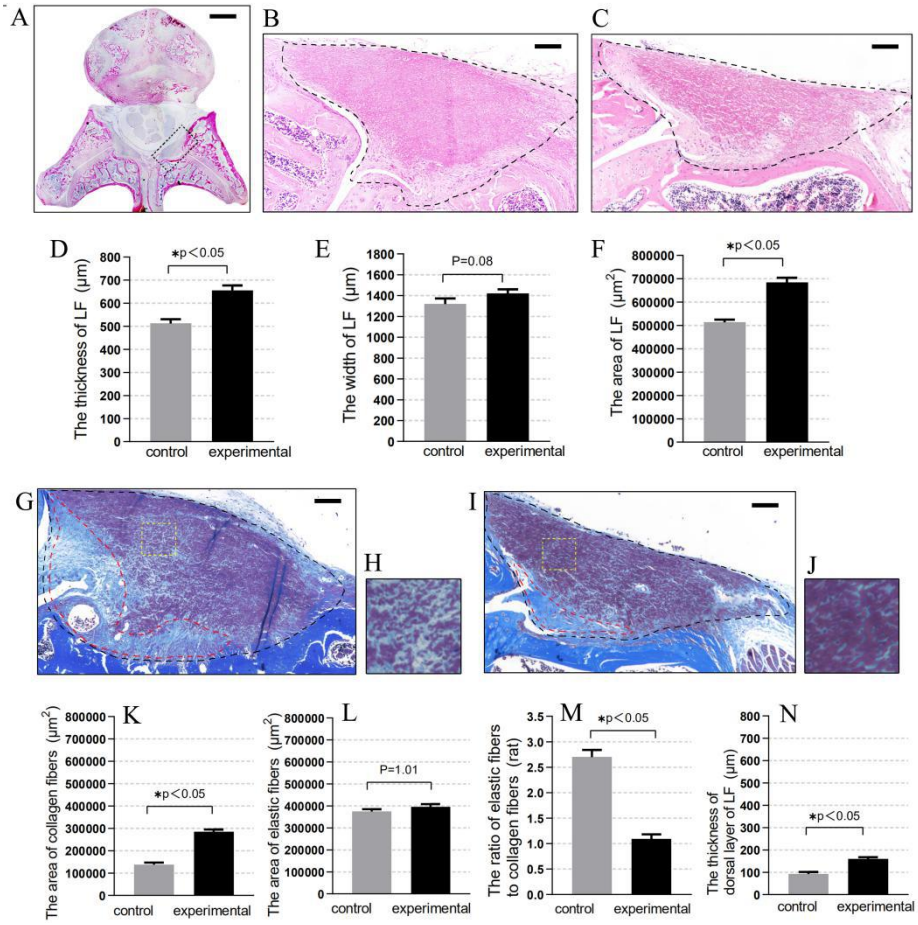

Fig 3. Lumbar instability induced LF hypertrophy on HE staining and on MT staining. (A) Axial sections of the rat lumbar spine. The cross-sectional area of LF in the experimental group and control group on HE staining were shown respectively in (B) and (C). The (D), (E), and (F) Bar graphs showing the thickness, width, and cross-sectional area in the two groups. The cross-sectional area of LF in the experimental group and control group on MT staining were shown respectively in (G) and (I). The fibrotic area were in the red circle. The (H) and (J) were high magnifications of (G) and (I). The (K) and (L) Bar graph showed the area of collagen fibers and elastic fibers in the two groups. The (M) Bar graph showed the ratio of elastic fibers to collagen fibers in the two groups. The (N) bar showed the thickness of dorsal layer of LF. *Scale bar, 500 and 100 μm for low (A) and high (B ,C ,G ,I) magnification images, respectively*

The histological analysis of human compared with rat

We compared the the severity of hypertrophy LF in the rat model and that in the human samples. In the human samples, we found non-hypertrophied LF showed a dense, continuous, and regular bundle of elastic fibers. In contrast, hypertrophied LF showed sparse, fragmented, and irregular elastic fibers on MT staining. The ratio of elastic fibers to collagen fibers also decreased in hypertrophied human LF compared to non-hypertrophied human LF. The severity of this histologically change was proportional to the LF thickness (Fig. 4a-d).

In rat model, the elastic fibers in the control group were dense which were similar to non-hypertrophied LF of human. Whereas the elastic fibers in the experimental group were sparse, slightly degenerated. The ratio of elastic-to-collagen fibers was 1.19±0.14 in the rats (Fig. 3m), which was similar to human mildly hypertrophied LF with the ratio of 1.08±0.09 (Fig. 4e). These results indicated that our rat model by lumbar instability was histologically identical to mildly hypertrophied LF of human.

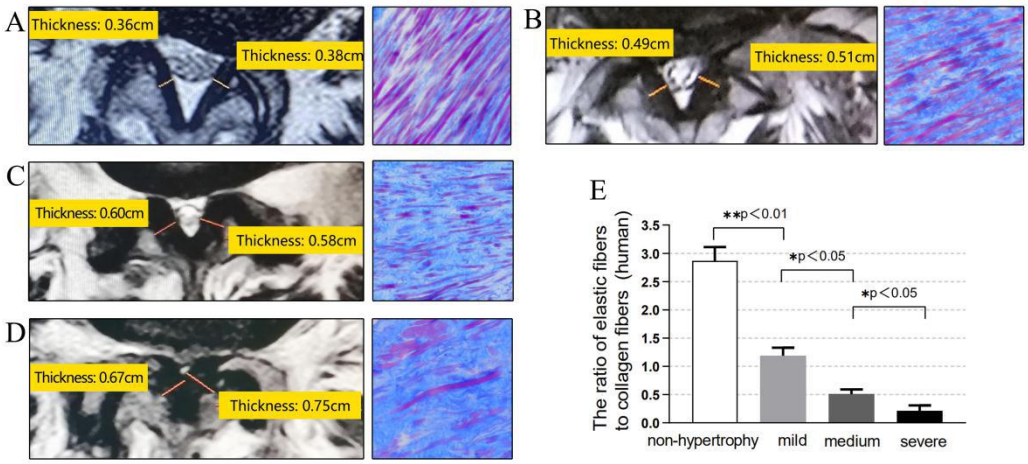

Fig 4. This rat model histologically identical to mildly hypertrophied LF of human. (A-D) image showed the MRI and MT staining of human samples: (A) non-hypertrophy, (B) mild hypertrophy, (C) medium hypertrophy, and (D) severe hypertrophy. The yellow lines indicated thickness of the LF. The (E) Bar graph showed the ratio of elastic fibers to collagen fibers in the four human groups.

The immunohistochemical and PCR analysis

The L5/6 level LF in model group had significantly larger optical density (OD value) of TGF-β1, IL-1β, and Col 1 than that on the same level in control group ($p < 0.05$, Fig. 5b). Representative specimens of TGF-β1, TNF-α, IL-1β, and Col 1 immunohistological staining are shown in Fig. 5a. we also evaluated the gene expression of TGF-β1, TNF-α, IL-1β, and Col 1 in both groups. The PCR analysis demonstrated that the gene expression of TGF-β1, TNF-α, IL-1β, and Col 1 were significantly higher in the experimental group than that in the control group ($p < 0.05$, Fig. 5C).

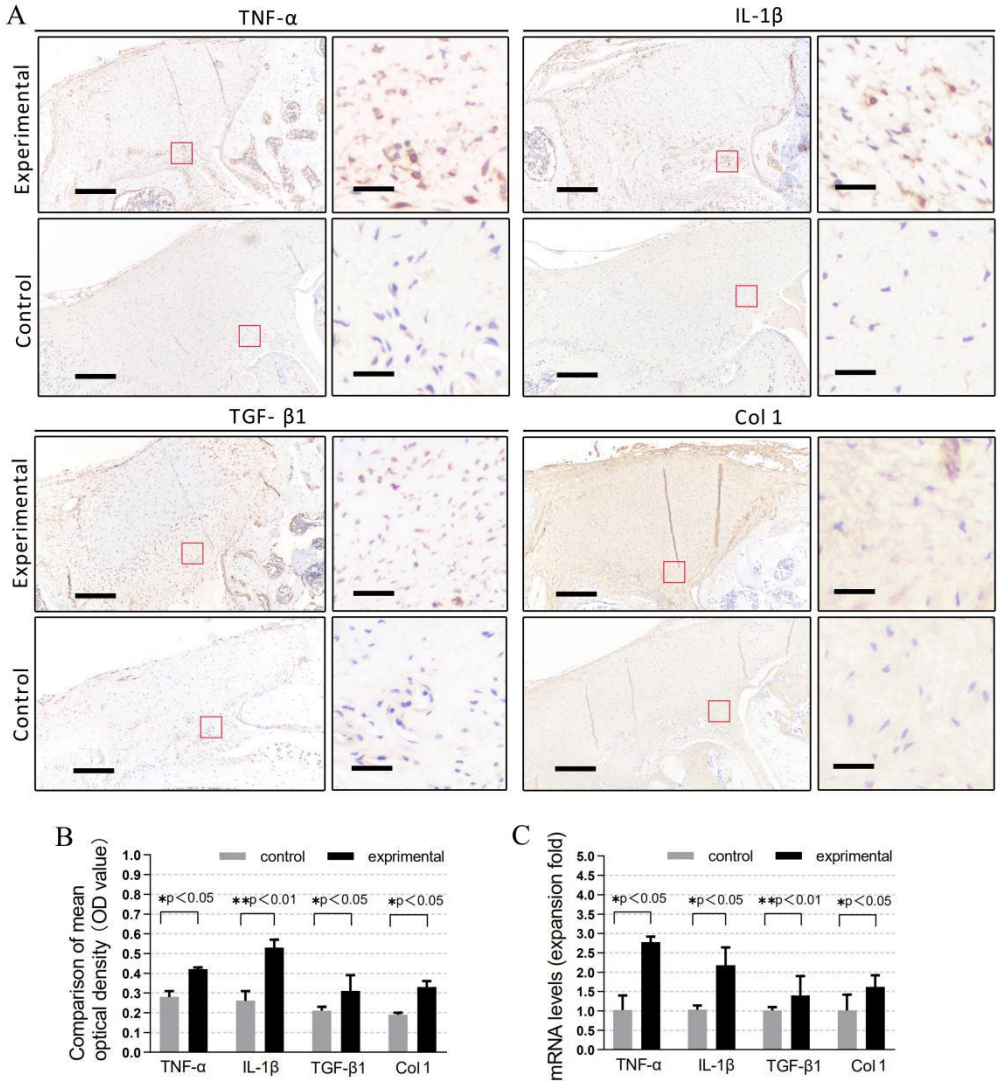

Fig. 5. (A) Immunohistochemistry of TGF-β1, IL-1β, and Col 1 in the L5/6 LF of the experimental and control group at 8 weeks after the surgery. Inset boxes in the left panels indicate the enlarged images in the right panels. (B) Comparison of mean optical density (OD value). (C) Comparison of mRNA levels (expansion fold). *Scale bar, 100 and 10 μm for low and high magnification images, respectively.*

Discussion

LF hypertrophy is one of the major factors of canal narrowing in LSCS. Spinal instability is thought to contribute to LF hypertrophy, but this pathophysiological mechanisms are still controversial. Therefore, we intend to elucidate the development of LF hypertrophy over a time course by lumbar instability of experimental rat. In this study, by applying posterior destabilization to the rat lumbar, we demonstrated that lumbar instability was one of the direct causes of LF hypertrophy. To our knowledge, no experimental investigation that could clarify the effect of lumbar instability on the LF has been carried out.

Previous study reported that the resection of spinous process, inter-and supraspinous ligaments, and facet joints caused lumbar instability and intervertebral disc degeneration (IDD) over a 12 weeks period in mice [16]. Biomechanical study using human or pig spines showed that instability of the motion segment was increased when lumbar facet joints, spinous process, and other posterior lumbar elements were resected [18-19]. In addition, paraspinal muscle removal surgery in a rabbit model can lead to cervical instability and LF degeneration [20]. Therefore, we hypothesized that the lumbar instability could lead to IDD and must be accompanied by LF

degeneration. Thus, we tried to resect both facet joints, spinous process with ligaments, and paraspinal muscle to concentrate much more stress on a certain lumbar segment, which was expected to induce lumbar LF hypertrophy within a short period.

Compared with previous studies using human specimens, we would be able to obtain more accurate data regarding the biological reaction of the LF to lumbar instability using a rat model. To assess whether the rat was a feasible experimental animal model for the study of LF hypertrophy, we evaluated histological results of the rat lumbar spine. In the axial sections of the lumbar spine, HE staining demonstrated that the rat LF was located between the dural sac and facet joints. In the sagittal sections, the LF ran between adjacent laminas. These histological features were very similar to those of human LF. Furthermore, the normal LF in humans is a well-defined elastic structure with 75% elastic fibres and 25% collagen fibres [6]. In this study, the density of elastic fibres with MT stain in control group was almost equal to that of the normal LF in humans. Based on these findings, the structure of the LF in rats was similar to that in humans. Therefore, using a rat model to examine the pathomechanism underlying LF hypertrophy for the study was considered reasonable.

The radiographical analyses showed wide disc space, increased range of motion and bony spur formation. Similar to our data, Fukui et al [13] found that increased disc height and endplate irregularities were observed at surgery segment after lumbar facetectomy in the rat. In contrast, the disc height decreased after lumbar facetectomy in the recent mouse IDD model [16]. The discrepancy between these models may be due to the difference of surgical procedures, position of X-ray (dynamic position VS. normal position), observation time points, or that of species (rat VS. mouse).

Furthermore, the increased expression of TGF-β1, IL-1β, TNF-α and Col 1 was similar to the previous results in human hypertrophied LF [8-9]. Inflammation-related gene expression such as COX-2, TNF-α, and IL-1, -6, -8, -15 were found in the human ligamentum flavum. Its expression showed weak positive linear correlation with the thickness of ligament [7]. Accumulation of fibrosis (scarring) caused hypertrophy of the ligamentum flavum. In fibrotic diseases of several organs, TGF-β1 has been reported to be an important disease related factor for collagen production and deposition [2]. In hypertrophied LF of humans, macrophages as well as vascular endothelial cells but not only fibroblasts showed a strong expression of TGF-β1 [22]. Sairyo et al [27] reported that the expression of TGF -β1 mRNA was higher in the early stage of the LF degeneration, but not in the later stage. Its expression decreased as the ligamentum flavum thickness increased. The over expression of TGF- β 1 might not completely cover the whole process of LF hypertrophy, which multiple factors involved. The expression of TGF -β1 is still controversial in present studies. Therefore, we should continue to explore the expression of this factor regarding to different stages of the hypertrophied LF in the future.

The epiligament constitutes the surface layer of ligaments and consists of woven bundles of collagen fibers [24]. Bray et al [25] also found that medial collateral ligament (MCL) hypertrophy of the epiligament induced MCL hypertrophy in the animal knee instability model. Thus, the epiligament can be considered to play a major role in ligament hypertrophy. In our study, posterior lumbar instability probably caused the thicken of the dorsal epiligament. This histological finding was similar to the human samples from the LSCS patients [26]. Sairyo et al [23] previously reported that mechanical stress at the dorsal aspect was about 5-fold higher than that at the dural aspect of the LF. Flexion is the most important motion for inducing mechanical stress in the LF. Higher mechanical stress at the dorsal aspect may induce micro injury in daily activities. During the process of micro injury healing, a thick fibrotic mass may be produced.

There are still several limitations in our study. We should note the facts that LF are not the same in rat and human in terms of their size, nutrition, and the biomechanical stress that they receive (less axial compression or torsion) [27]. These differences should be considered in judging the results obtained from the present model. Furthermore, due to the ratio of the LF to the dural tube was significantly smaller in rat than in humans. Our lumbar

instability rat model can not be used to develop an LSCS model. Nevertheless, we believe that our model established in this study partly showed the pathological features of human hypertrophied LF, and is very helpful for us to understand its pathological process and mechanism.

Conclusion

In conclusion, we demonstrated for the first time that lumbar instability directly induced LF hypertrophy in a reproducible rat model. In addition, lumbar instability could lead to high expression of inflammatory and fibrotic factors in LF, causing the accumulation of collagen fibers and decreasing of elastic fibers.

Abbreviations

LSCS: Lumbar spinal canal stenosis; LF: ligamentum flavum; IL-1β: Interleukin-1; TNF-α: Tumor Necrosis Factor; TGF-β1: Transforming Growth Factor-β1; Col 1: Collagen 1; DHR: Disc height ratios; A: Anterior; M: middle; P: posterior; MRI: magnetic resonance imaging; HE: ematoxylin-eosin; MT: Masson trichrome; MOD: mean optical density; ECM: extracellular matrix; IDD: intervertebral disc degeneration; MCL: medial collateral ligament

Authors' contributions

BJW and CYG: performing rat experiment, acquisition of the data, data analysis, and writing the manuscript. PZ and JRZ: histological analysis, immunohistological evaluation, and real-time PCR analysis. WS and CYG: collection of human LF samples. JHG, PZ, XW, and LGZ: design of the study. All authors reviewed the manuscript.

Funding

This work was supported by the National Natural Science Foundation of China (Grant no. 81473694). The funders had no role in the design of the study, data collection, analysis, interpretation of data, in writing the manuscript, or decision to publish.

Availability of data and materials

The datasets used and/or analysed during the current study are available from the corresponding author on reasonable request.

Ethics approval and consent to participate

This study protocol on human was approved by the Ethics Committee of Wangjing hospital, Chinese Academy of traditional Chinese Medicine (No. WJEC-YJS-2020-009-P002) and all procedures were performed according to the Declaration of Helsinki. Participants provided consent with an approved informed consent document before enrollment in the study. This study protocol on rats was approved by the Animal Ethics Committee of the Institute of Basic Theory for Chinese Medicine, China Academy of Chinese Medical Sciences and was compliant with NIH guidelines for the humane care and use of laboratory animals. All methods were carried out in accordance with ARRIVE guidelines.

Consent for publication

Not Applicable.

Competing interests

The authors declare that they have no competing interests.

Author details

[1]Department of Spine, Wangjing Hospital of China Academy of Chinese Medical Sciences, Beijing, China. [2]Department of Pathology, Wangjing Hospital of China Academy of Chinese Medical Sciences, Beijing, China.

Funding

This study was supported by the National Natural Science Foundation of China (No.81473694).

Acknowledgments

The authors would like to thank Jian-guo Li, Lu-guang Li, and Wei Yang for performing rat experiment.

References

1. Szpalski M, Gunzburg R. Lumbar spinal stenosis in the elderly: an overview. Eur Spine J. 2003; 12:S170-5.
2. Kalichman L, Cole R, Kim DH, Li L, Suri P, Guermazi A, Hunter DJ. Spinal stenosis prevalence and association with symptoms: the Framingham Study. Spine J. 2009;9(7):545-50.
3. Iwahashi H, Yoshimura N, Hashizume H, Yamada H, Oka H, Matsudaira K, Shinto K, Ishimoto Y, Nagata K, Teraguchi M, et al. The Association between the Cross-Sectional Area of the Dural Sac and Low Back Pain in a Large Population: The Wakayama Spine Study. PLoS One. 2016;11(8):e0160002.
4. Towne EB, Reichert FL. Compression of the Lumbosacral Roots of the Spinal Cord by Thickened Ligamenta Flava. Ann Surg. 1931;94(3):327-36.
5. Okuda T, Baba I, Fujimoto Y, Tanaka N, Sumida T, Manabe H, Hayashi Y, Ochi M. The pathology of ligamentum flavum in degenerative lumbar disease. Spine (Phila Pa 1976). 2004;29(15):1689-97.
6. Kosaka H, Sairyo K, Biyani A, Leaman D, Yeasting R, Higashino K, Sakai T, Katoh S, Sano T, Goel VK, et al. Pathomechanism of loss of elasticity and hypertrophy of lumbar ligamentum flavum in elderly patients with lumbar spinal canal stenosis. Spine (Phila Pa 1976). 2007;32(25):2805-11.
7. Sairyo K, Biyani A, Goel VK, Leaman DW, Booth R Jr, Thomas J, Ebraheim NA, Cowgill IA, Mohan SE. Lumbar ligamentum flavum hypertrophy is due to accumulation of inflammation-related scar tissue. Spine (Phila Pa 1976). 2007;32(11):E340-7.
8. Moon HJ, Park YK, Ryu Y, Kim JH, Kwon TH, Chung HS, Kim JH. The angiogenic capacity from ligamentum flavum subsequent to inflammation: a critical component of the pathomechanism of hypertrophy. Spine (Phila Pa 1976). 2012;37(3):E147-55.
9. Park JB, Chang H, Lee JK. Quantitative analysis of transforming growth factor-beta 1 in ligamentum flavum of lumbar spinal stenosis and disc herniation. Spine (Phila Pa 1976). 2001;26(21):E492-5.
10. Hur JW, Kim BJ, Park JH, Kim JH, Park YK, Kwon TH, Moon HJ. The Mechanism of Ligamentum Flavum Hypertrophy: Introducing Angiogenesis as a Critical Link That Couples Mechanical Stress and Hypertrophy. Neurosurgery. 2015;77(2):274-81.
11. Yabe Y, Hagiwara Y, Ando A, Tsuchiya M, Minowa T, Takemura T, Honda M, Hatori K, Sonofuchi K, Kanazawa K, et al. Chondrogenic and fibrotic process in the ligamentum flavum of patients with lumbar spinal canal stenosis. Spine (Phila Pa 1976). 2015;40(7):429-35.
12. Yoshiiwa T, Miyazaki M, Notani N, Ishihara T, Kawano M, Tsumura H. Analysis of the Relationship between Ligamentum Flavum Thickening and Lumbar Segmental Instability, Disc Degeneration, and Facet Joint Osteoarthritis in Lumbar Spinal Stenosis. Asian Spine J. 2016;10(6):1132-1140.
13. Fukui D, Kawakami M, Yoshida M, Nakao S, Matsuoka T, Yamada H. Gait abnormality due to spinal instability after lumbar facetectomy in the rat. Eur Spine J. 2015;24(9):2085-94.
14. Fukui D, Kawakami M, Cheng K, Murata K, Yamada K, Sato R, Yoshida M, Yamada H, Inoue N, Masuda K.

Three-dimensional micro-computed tomography analysis for spinal instability after lumbar facetectomy in the rat. Eur Spine J. 2017;26(8):2014-2020.
15. Norcross JP, Lester GE, Weinhold P, Dahners LE. An in vivo model of degenerative disc disease. J Orthop Res. 2003;21(1):183-8.
16. Oichi T, Taniguchi Y, Soma K, Chang SH, Yano F, Tanaka S, Saito T. A Mouse Intervertebral Disc Degeneration Model by Surgically Induced Instability. Spine (Phila Pa 1976). 2018;43(10):E557-E564.
17. Kim YU, Park JY, Kim DH, Karm MH, Lee JY, Yoo JI, Chon SW, Suh JH. The Role of the Ligamentum Flavum Area as a Morphological Parameter of Lumbar Central Spinal Stenosis. Pain Physician. 2017;20(3):E419-24.
18. Abumi K, Panjabi MM, Kramer KM, Duranceau J, Oxland T, Crisco JJ. Biomechanical evaluation of lumbar spinal stability after graded facetectomies. Spine (Phila Pa 1976). 1990;15(11):1142-7.
19. Gillespie KA, Dickey JP. Biomechanical role of lumbar spine ligaments in flexion and extension: determination using a parallel linkage robot and a porcine model. Spine (Phila Pa 1976). 2004;29(11):1208-16.
20. Xishan Zhang, Xihai Fan, Yanming Zhang. Experimental studies on ultra-micro structure of ligamentum flavum at early degeneration.Orthopedic Journal of China. 2009;17(17):1344-7.
21. Li J, Campanale NV, Liang RJ, Deane JA, Bertram JF, Ricardo SD. Inhibition of p38 mitogen-activated protein kinase and transforming growth factor-beta1/Smad signaling pathways modulates the development of fibrosis in adriamycin-induced nephropathy. Am J Pathol. 2006;169(5):1527-40.
22. Löhr M, Hampl JA, Lee JY, Ernestus RI, Deckert M, Stenzel W. Hypertrophy of the lumbar ligamentum flavum is associated with inflammation-related TGF-β expression. Acta Neurochir (Wien). 2011;153(1):134-41.
23. Sairyo K, Biyani A, Goel V, Leaman D, Booth R Jr, Thomas J, Gehling D, Vishnubhotla L, Long R, Ebraheim N. Pathomechanism of ligamentum flavum hypertrophy: a multidisciplinary investigation based on clinical, biomechanical, histologic, and biologic assessments. Spine (Phila Pa 1976). 2005;30(23):2649-56.
24. Frank CB. Ligament structure, physiology and function. J Musculoskelet Neuronal Interact. 2004;4(2):199-201.
25. Bray RC, Fisher AW, Frank CB. Fine vascular anatomy of adult rabbit knee ligaments. J Anat. 1990;172:69-79.
26. Sato N, Higashino K, Sakai T, Terai T, Goel VK, Biyani A, Ebraheim N, Takata Y, Hayashi F, Yamashita K, et al. Role of Epiligament in Ligamentum Flavum Hypertrophy in Patients with Lumbar Spinal Canal Stenosis:a Pilot Study. J Med Invest. 2018;65(1.2):85-89.
27. Larson JW 3rd, Levicoff EA, Gilbertson LG, Kang JD. Biologic modification of animal models of intervertebral disc degeneration. J Bone Joint Surg Am. 2006;88(S2):83-7.

Figures

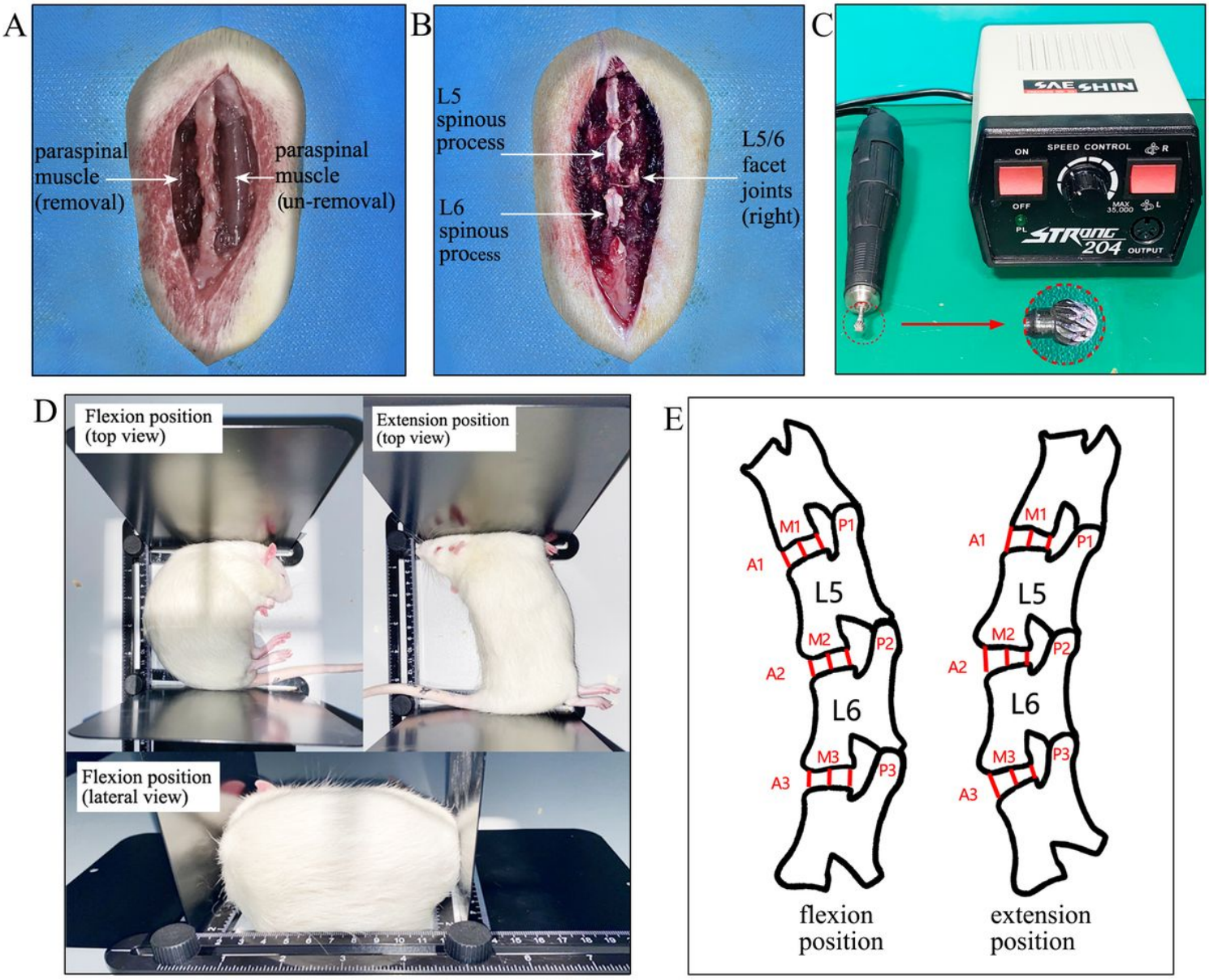

Figure 1

Surgical procedures and radiological methods. (A) Removal of L5-L6 paraspinal muscle. (B) Complete resection of L5 and L6 spinous process, semi-grinding of the bilateral L5/6 facet joints. (C) A Grinder and round drill bit used to semi-grind the facet joints.(D)Overextension and flexion position of rats using are tractable holder. (E) Measurement indicators: (1) Disc height ratios (DHR) in flexion and extension were calculated as follows: anterior DHR =2×A2/(A1+A3), middle DHR = 2×M2/(M1+M3), posterior DHR =2×P2/(P1 +P3). (2)Flexion and extension ratios were calculated as follows: flexion ratio = A2/P2 in flexion, extension ratio = A2/P2 in extension. A anterior, M middle, P posterior.

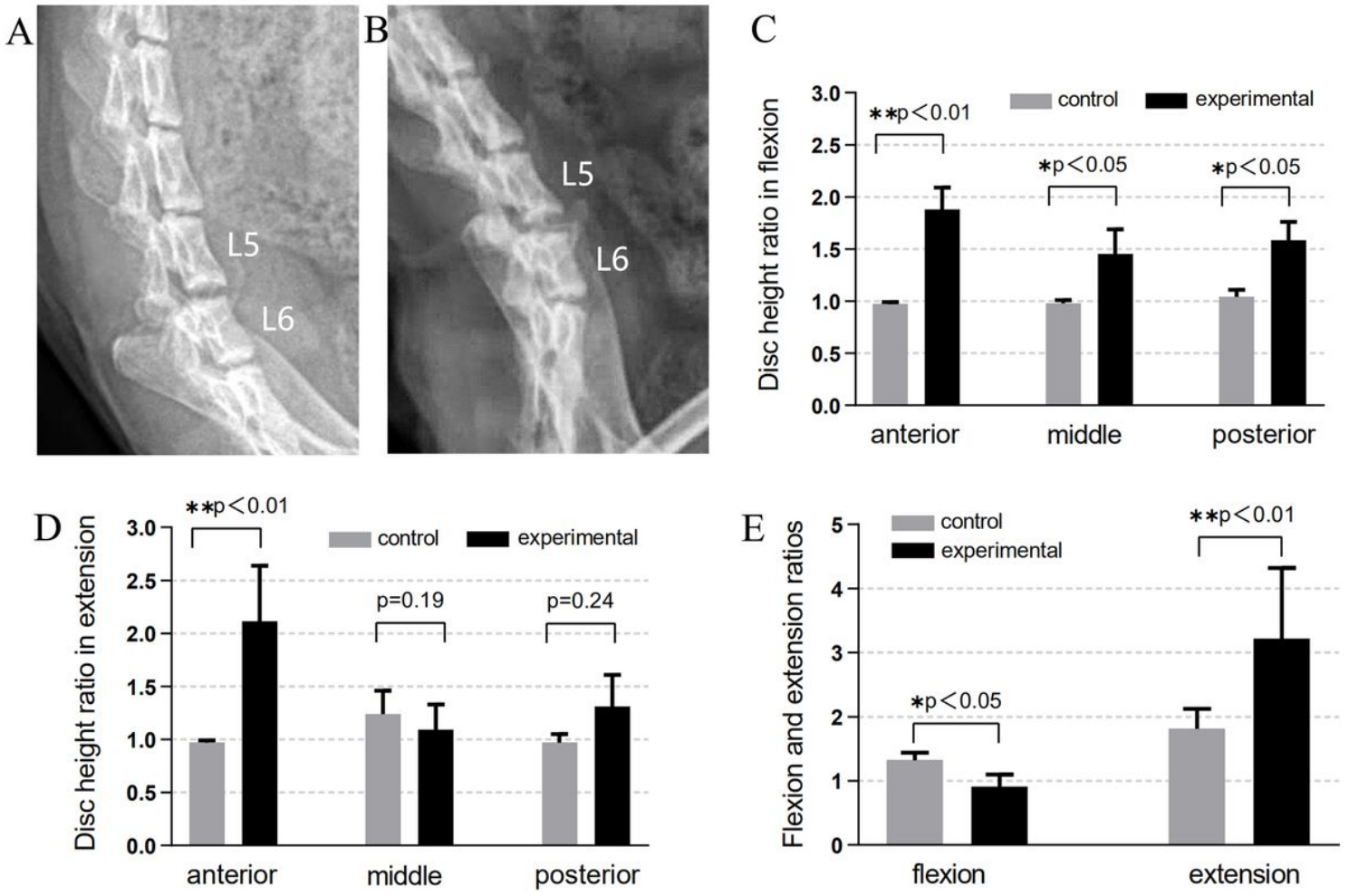

Figure 2

Radiological analysis at 8 weeks postoperatively. Wide disc space and anterior osteophyte formation was found on L5/6 of (A) flexion position and (B) flexion position on lateral radiographs. (C) The disc height ratio of the flexion position was larger in the rats in the experimental group than in the rats in the control groups. (D) The anterior disc height ratio of the extension position was larger in the rats in the experimental group than in the rats in the control groups. (E) The extension ratios were larger in the rats in the experimental group than in the rats in the control groups.

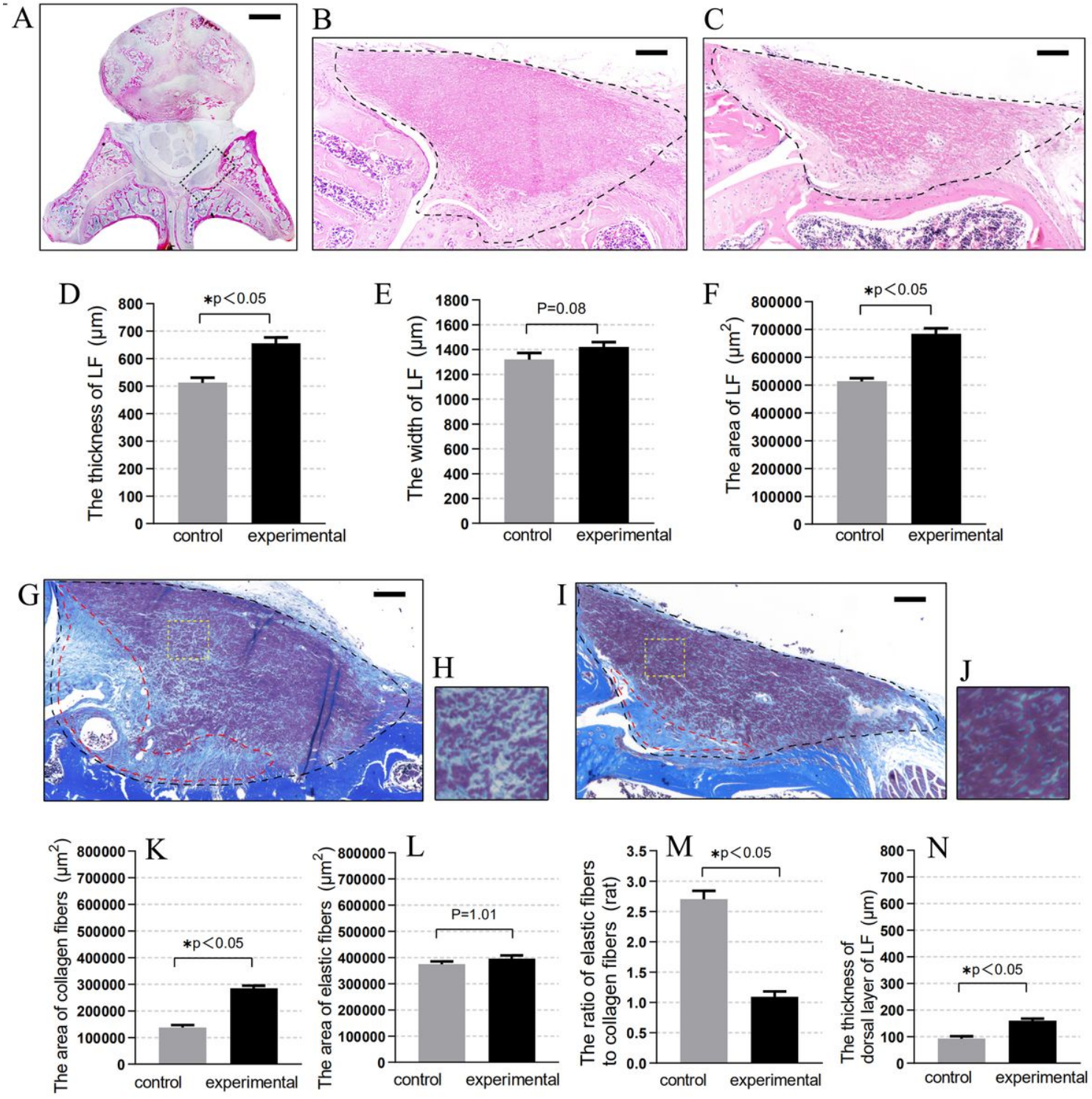

Figure 3

Lumbar instability induced LF hypertrophy on HE staining and on MT staining. (A) Axial sections of the rat lumbar spine. The cross-sectional area of LF in the experimental group and control group on HE staining were shown respectively in (B) and (C). The (D), (E), and (F) Bar graphs showing the thickness, width, and cross-sectional area in the two groups. The cross-sectional area of LF in the experimental group and control group on MT staining were shown respectively in (G) and (I). The fibrotic area were in the red circle. The (H) and (J) were high magnifications of (G) and (I). The (K) and (L) Bar graph showed

the area of collagen fibers and elastic fibers in the two groups. The (M) Bar graph showed the ratio of elastic fibers to collagen fibers in the two groups. The (N) bar showed the thickness of dorsal layer of LF. Scale bar, 500 and 100 μm for low (A) and high (B ,C ,G ,I) magnification images, respectively

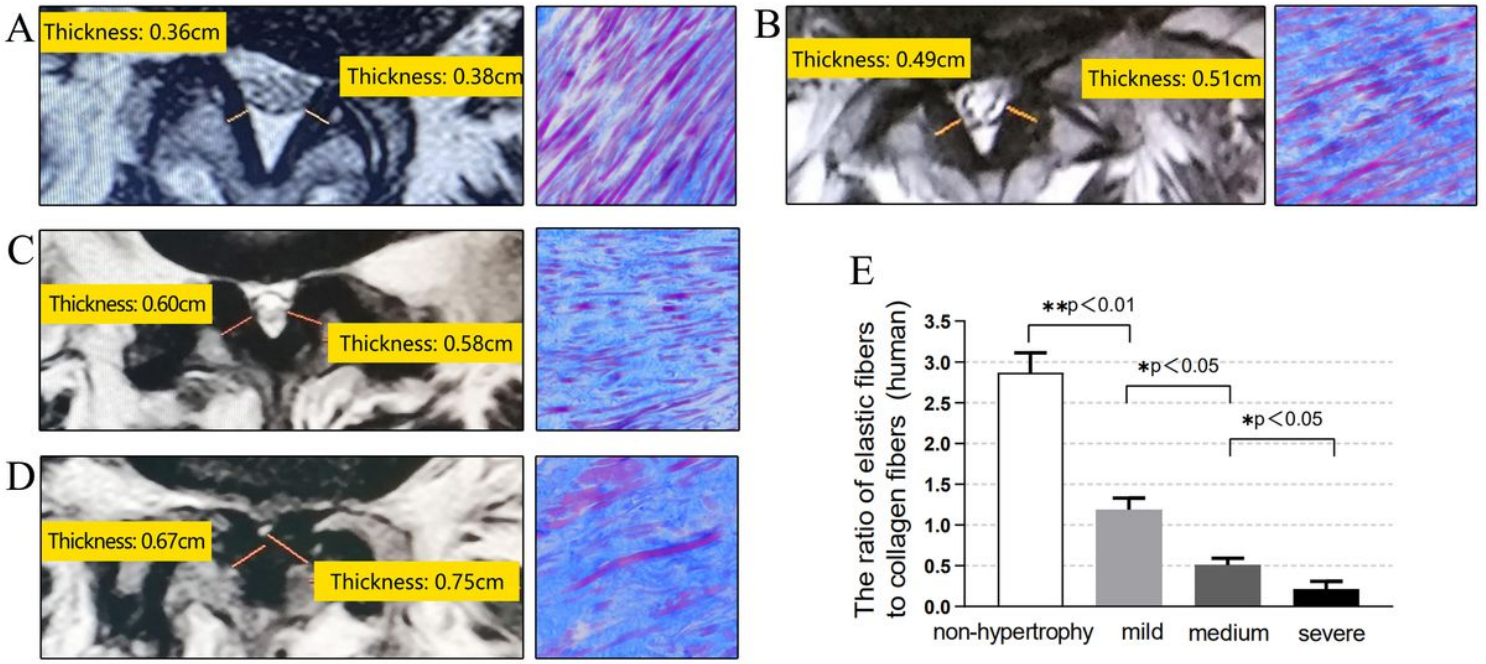

Figure 4

This rat model histologically identical to mildly hypertrophied LF of human. (A-D) image showed the MRI and MT staining of human samples: (A) non-hypertrophy, (B) mild hypertrophy, (C) medium hypertrophy, and (D) severe hypertrophy. The yellow lines indicated thickness of the LF. The (E) Bar graph showed the ratio of elastic fibers to collagen fibers in the four human groups.

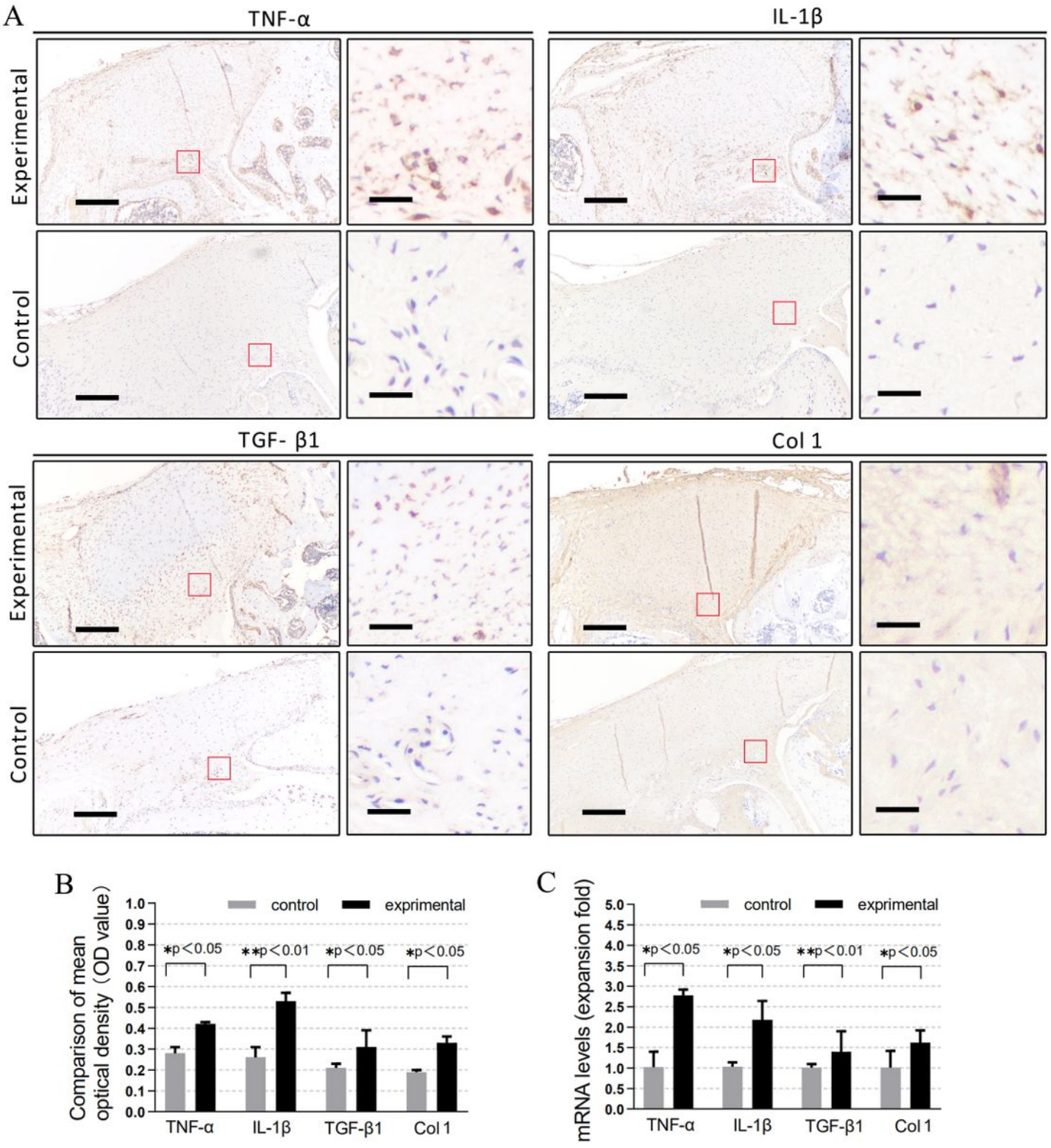

Figure 5

(A) Immunohistochemistry of TGF-β1, IL-1β, and Col 1 in the L5/6 LF of the experimental and control2 09 group at weeks after the surgery. Inset boxes in the left panels indicate the enlarged images in the right panels.(B) Comparison of mean optical density (OD value). (C) Comparison of mRNA levels (expansion fold). Scale bar, 100 and 10μm for low and high magnification images, respectively.